coatings

MDPI

Article

Water-Developable PFAS-Free Glycan-Derived Positive Photoresist Materials for Environmentally Friendly Lithography

Yuna Hachikubo [1], Hiryu Hayashi [1], Mano Ando [1], Mayu Morita [1], Misaki Oshima [1], Abdul Manaf Hashim [2], Nurul Hanis Azhan [2], Takayuki Ota [3] and Satoshi Takei [1,*]

[1] Graduate School of Engineering, Toyama Prefectural University, Imizu 939-0398, Toyama, Japan; y.hachikubo@outlook.com (Y.H.); hiryu0821@outlook.jp (H.H.); mano_ando@outlook.jp (M.A.); mayu_.morita@outlook.jp (M.M.); misaki_oshima@outlook.jp (M.O.)
[2] Malaysia-Japan International Institute of Technology, Universiti Teknologi Malaysia, Kuala Lumpur 54100, Malaysia; abdmanaf@utm.my (A.M.H.); nurulhanis.a@utm.my (N.H.A.)
[3] Gunei Chemical Industry, Takasaki 370-0032, Gunma, Japan; t-ota@gunei-chemical.co.jp
* Correspondence: takeis@pu-toyama.ac.jp

Abstract

Traditional lithography processes use resist materials that require organic solvents during the development step but also often contain components derived from PFASs (per- and polyfluoroalkyl substances), raising concerns about environmental pollution and sustainability. PFASs are difficult to degrade, and their long-term effects on ecosystems and human health are the subject of international concern, making the development of alternative technologies an urgent priority. Lithography is a fundamental technology with applications beyond semiconductor manufacturing, electronics, biomedicine, and microfluidic devices. Addressing its environmental impact remains critical in both academic and industrial contexts. This study introduces a water-developable positive photoresist derived from a polymeric material incorporating plant-derived sugar chains as the resist backbone. The reactivity of the material to ultraviolet irradiation, enabled by a photoacid generator, allows microfabrication through water development. Moreover, successful micrometer-scale patterning demonstrated a superior resolution compared to previous sugar-derived water-developable resists. The dextrin-based resist exhibited the highest performance, achieving a sensitivity of 150 mJ/cm^2 and a resolution of 3.6 µm under an environmentally benign, PFAS-free process that enabled development with water. These findings propose a sustainable alternative to conventional petrochemical-derived photoresists, positioning it as a promising candidate for environmentally friendly photolithography processes.

Keywords: water-based development; PFAS-free; eco-friendly; microfabrication; photolithography; biomass-derived

check for updates

Academic Editor: Je Moon Yun

Received: 26 September 2025
Revised: 16 October 2025
Accepted: 17 October 2025
Published: 20 October 2025

Citation: Hachikubo, Y.; Hayashi, H.; Ando, M.; Morita, M.; Oshima, M.; Hashim, A.M.; Azhan, N.H.; Ota, T.; Takei, S. Water-Developable PFAS-Free Glycan-Derived Positive Photoresist Materials for Environmentally Friendly Lithography. *Coatings* **2025**, *15*, 1228. https://doi.org/10.3390/coatings15101228

Copyright: © 2025 by the authors. Licensee MDPI, Basel, Switzerland. This article is an open access article distributed under the terms and conditions of the Creative Commons Attribution (CC BY) license (https://creativecommons.org/licenses/by/4.0/).

1. Introduction

In recent years, the pursuit of a carbon-neutral society and advancement of the circular economy [1] have underscored the urgent need for the development of sustainable materials that minimize environmental impact while reducing reliance on petroleum resources [2–4]. In this context, bio-based polymers derived from renewable resources have garnered significant attention because of their biodegradability and potential to reduce CO_2 emissions. These polymers are increasingly being applied across diverse fields, including packaging materials, medical hydrogels, adhesives, and coating agents [5–8]. Notably, natural polymers such as starch, cellulose, and chitosan, which possess glycan structures,

offer abundant raw materials and flexibility in molecular design, positioning them as promising candidates for next-generation high-performance, environmentally compatible materials [9,10]. Concurrently, micro- and nanofabrication technologies, including photolithography, have evolved primarily within the semiconductor industry. Recently, these technologies have rapidly advanced in the life sciences domain, encompassing areas such as regenerative medicine [11], cell engineering [12,13], microfluidics [14], and biosensors [15]. For instance, technologies have been developed to spatially control biological behaviors, such as cell adhesion, differentiation, and polarity formation, by creating micropatterns on substrate surfaces [16–18]. These advancements are crucial for constructing reproducible in vitro cell models and for fabricating three-dimensional tissue models [19,20].

Contact-based processes, such as soft lithography [21] and stamp replication, have been widely employed to directly impart fine structures onto biomaterials. However, these methods face challenges, including limited transfer accuracy, defects during stamp detachment, and low throughput [22]. In contrast, photolithography technology offers non-contact, high-speed, and high-precision pattern formation, making it a promising alternative, particularly for microfabrication and bio-device manufacturing applications. Nevertheless, many photosensitive polymers (photoresists) used in this process are petroleum-derived and necessitate organic solvent spin coating, as well as strong alkaline developing solutions such as tetramethylammonium hydroxide (TMAH). TMAH exhibits central nervous system toxicity and skin corrosivity, and its waste liquid disposal requires stringent management, posing significant environmental burdens and serious health risks to workers [23]. Consequently, the development of water-developable resist materials using naturally derived materials is progressing [24]. For water-developable positive-type resists, Park et al. developed a water-developable resist using silk fibroin [25], and Servin et al. developed a resist using chitosan and performed deep ultraviolet (DUV) lithography [26].

Furthermore, in addition to TMAH, organic fluorine compounds (PFAS) [27], which have been introduced to enhance resist performance, are extensively utilized because of their properties, such as water repellency and low surface tension. However, recent years have seen increasing concerns regarding their environmental persistence, bioaccumulation, and toxicity, prompting a trend toward more stringent regulatory enforcement, particularly in Europe [28,29]. Consequently, the development of photoresists based on natural materials that are compatible with water treatment processes and do not incorporate petroleum-derived components, PFAS, or TMAH has emerged as an international research challenge [30,31]. Against this backdrop, a previous study conducted in our laboratory involved the development of a water-developable resist using a glycan structure as the negative-type material, with photolithography performed using a high-pressure mercury lamp [32] and i-line exposure [33]. However, with negative-type materials, the exposed areas cross-link and remain, rendering the patterns more susceptible to swelling and edge blurring than positive-type materials.

Therefore, this study aimed to develop a positive-type water-developable resist material utilizing high-pressure mercury lamps, which are more accessible than DUV due to their lower cost and greater compatibility with various equipment and materials. By focusing on sugar chains among naturally derived materials, we designed and synthesized a positive photoresist material compatible with water development and free of PFAS by introducing photoreactive functional groups into the resin. This glycan-based resist features a chemical structure that is altered upon UV irradiation, enabling the formation of fine patterns through water development alone.

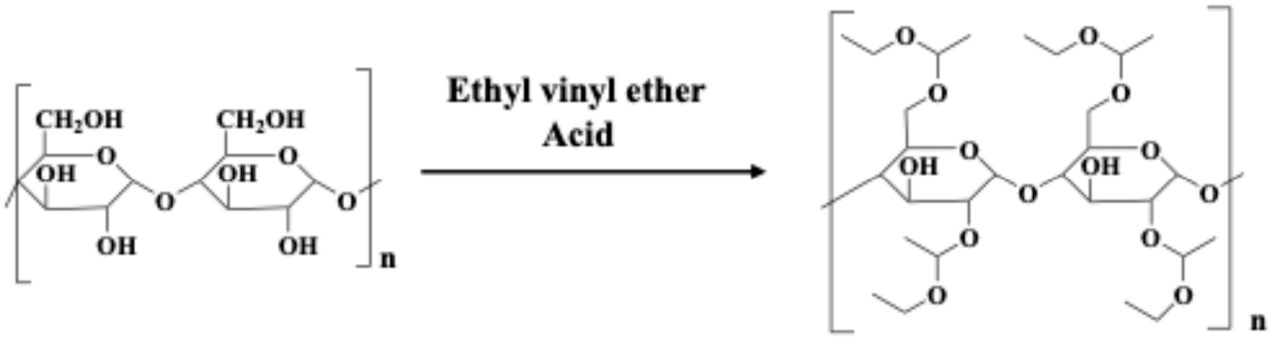
2. Materials and Methods

2.1. Raw Materials

The raw materials used for the experiments included dextrin [NSD500S, $(C_6H_{10}O_5)_n$], supplied by San-ei Sugar Co., Ltd. (Aichi, Japan), and resistant dextrin [FiberSol-2, $(C_6H_{10}O_5)_n$], obtained from Matsutani Chemical Industry Co., Ltd. (Hyogo, Japan); ethyl vinyl ether (EVE, C_4H_8O, purity $\geq$ 99%), purchased from BASF (Ludwigshafen am Rhein, Germany). N-Methylpyrrolidone (NMP, C_5H_9NO, purity $\geq$ 99.9%) was purchased from Mitsubishi Chemical Corp. (Tokyo, Japan), and trifluoroacetic acid ($C_2HF_3O_2$, purity $\geq$ 98%) was obtained from FUJIFILM Wako Pure Chemical Corp. (Osaka, Japan). Triethylamine ($C_6H_{15}N$, 100%) was purchased from Daicel Corp. (Osaka, Japan). Methyl isobutyl ketone (MIBK, $C_6H_{12}O$, purity $\geq$ 99%) and propylene glycol monomethyl ether acetate (PGMEA, $C_6H_{12}O_3$, purity $\geq$ 99%) were supplied by Mitsui Chemicals, Inc. (Tokyo, Japan) and Daicel Corp. (Osaka, Japan), respectively. Triphenylsulfonium trifluoromethanesulfonate ($C_{19}H_{15}F_3O_3S_2$, purity $\geq$ 98%) was purchased from Tokyo Chemical Industry Co., Ltd. (Tokyo, Japan), and n-octylamine ($C_8H_{19}N$, purity $\geq$ 98%) was obtained from FUJIFILM Wako Pure Chemical Corp. (Osaka, Japan).

2.2. Synthesis of Positive-Type Water-Developable Resist

EVE was incorporated into the glycan structure to introduce a protective group, resulting in a positive-type water-developable resist, as illustrated in Scheme 1. Two distinct resist skeletons and four compounds with varying protection rates were synthesized. Additionally, eight samples were prepared to optimize the proportions of the photoacid generator (PAG) and acid quencher. The preparation methods for these samples are described below.



Scheme 1. Synthesis of glycan-derived positive-type water-developable resist.

2.2.1. Synthesis of Dextrin Based Resist, 80% Protection Rate

Initially, a reaction vessel equipped with a thermometer, stirrer, and cooling tube was prepared. NSD500S (20.9 wt%, 25.0 g) and NMP (48.7 wt%, 58.3 g) were introduced into the reaction vessel to form a solution. Subsequently, water was removed from the solution under vacuum conditions of −740 mmHg and at a temperature of 50 °C. The solution was then cooled to 30 °C and purged with nitrogen gas. Using this solution as the reaction medium, trifluoroacetic acid (4.4 wt%, 5.28 g, 0.046 mol) was added, followed by dropwise addition of EVE (22.1 wt%, 26.5 g, 0.368 mol) over one hour. The reaction was continued for three hours while maintaining the solution temperature at 30 °C. Triethylamine (3.9 wt%, 4.65 g, 0.046 mol) was added to neutralize the reaction mixture. MIBK and ion-exchanged water were added to the neutralized reaction mixture, transferring the neutralization salt and NMP to the aqueous phase, thereby purifying the product, which was an 80% acetal-modified dextrin. Under a vacuum of −740 mmHg, the mixture was heated to approximately 70 °C to concentrate the phase containing MIBK. Subsequently, the solvent was replaced with PGMEA, yielding a solution (hereafter referred to as D80) containing 80% acetal-modified dextrin at

a concentration of 15 wt%. Acetal-modified dextrin in D80 was considered to be 100 parts by weight. Triphenylsulfonium trifluoromethanesulfonate, a PAG, equivalent to 5.0 parts by weight, and n-octylamine, an acid quencher, equivalent to 0.5 parts by weight, were added to prepare photosensitive composition D80-5. Additionally, PAG equivalent to 10.0 parts by weight and an acid quencher equivalent to 1.0 part by weight were added to the acetal-modified dextrin in D80 at 100 parts by weight to prepare photosensitive composition D80-10.

2.2.2. Synthesis of Dextrin Based Resist, 100% Protection Rate

Except for altering the amount of EVE to 0.460 mol, the same procedure as D80 was employed to acetalize dextrin (NSD500S), producing a solution (hereafter referred to as D100) containing 15 wt% of the 100% acetal-modified dextrin. Acetal-modified dextrin in D100 was considered as 100 parts by weight, to which PAG equivalent to 5.0 parts by weight and an acid quencher equivalent to 0.5 parts by weight were added, thereby preparing photosensitive composition D100-5. Furthermore, with the acetal-modified dextrin in D100 as 100 parts by weight, 10.0 parts by weight of PAG, and 1.0 part by weight of acid quencher were added, thereby preparing photosensitive composition D100-10.

2.2.3. Synthesis of Indigestible Dextrin Based Resist, 80% Protection Rate

The synthesis procedure was identical to that of D80, except for the substitution of NSD500S with FiberSol 2. This resulted in a solution, hereafter referred to as IDex80, containing 15% by weight of 80% acetal-modified indigestible dextrin. The acetal-modified material in IDex80 was standardized to 100 parts by weight, to which 5.0 parts by weight of PAG and 0.5 parts by weight of an acid quencher were added to form photosensitive composition IDex80-5. Additionally, with the acetal-modified material in IDex80 at 100 parts by weight, 10.0 parts by weight of PAG and 1.0 part by weight of an acid quencher were incorporated, resulting in photosensitive composition IDex80-10.

2.2.4. Synthesis of Indigestible Dextrin Based Resist, 100% Protection Rate

The procedure was consistent with that of IDex80, except for the adjustment of ethyl vinyl ether to 0.460 mol, leading to the acetalization of indigestible dextrin (FiberSol 2). This yielded a solution, hereafter referred to as IDex100, containing 15% by weight of 100%-acetal-modified indigestible dextrin. The acetal-modified indigestible dextrin in IDex100 was standardized to 100 parts by weight, to which 5.0 parts by weight of PAG and 0.5 parts by weight of an acid quencher were added, forming the photosensitive composition IDex100-5. Furthermore, with 100 parts by weight of the acetal-modified indigestible dextrin in IDex100, 10.0 parts by weight of PAG and 1.0 part by weight of an acid quencher were incorporated, resulting in photosensitive composition IDex100-10. The compositions of the eight samples, prepared by varying the amounts of PAG and acid quencher in compounds D80, D100, IDex80, and IDex100, are summarized in Table 1.

Table 1. Composition of the created sample.

Samples		Resist Backbone	Protective Group Addition Amount (%)	PAG Addition Amount (%)	Quencher Addition Amount (%)
D80	D80-5	Dextrin	80	5	0.5
	D80-10			10	1
D100	D100-5		100	5	0.5
	D100-10			10	1
IDex80	IDex80-5	Indigestible dextrin	80	5	0.5
	IDex80-10			10	1
IDex100	IDex100-5		100	5	0.5
	IDex100-10			10	1

2.3. Chemical Analysis of Materials

Using a nuclear magnetic resonance spectrometer (JEOL RESONANCE, ECZ-500R/S1, Tokyo, Japan), ^{13}C-NMR measurements were performed to ascertain the modification rate of the protecting group for the hydroxyl group in the material. The sample was dissolved in THF using GPC (TOSOH EcoSEC HLC-8320PG, Tokyo, Japan) and adjusted to a concentration of 1% (w/v). Filtration was conducted using a 0.45 μm filter, followed by GPC measurement to determine the weight-average molecular weight (Mw). In addition, the average film thickness after spin coating and baking was measured to confirm the variations in the film thickness based on the molecular weight. For D80-10, structural changes before and after exposure were confirmed using attenuated total reflection Fourier-transform infrared spectroscopy (ATR-FTIR) of the infrared absorption spectra. FT-IR spectra were acquired using a Fourier-transform infrared spectrophotometer (Spectrum Two, PerkinElmer, Shelton, CT, USA) for both unexposed and 175 mJ/cm^2 exposed D80-10 samples.

2.4. Material Property Measurement

2.4.1. Measurement of Affinity Between Resist and Substrate

To assess the conditions for substrate treatment, static contact angle measurements were conducted using a fully automated contact angle measurement device (Dropmaster DM500, Kyowa Surface Science Co., Ltd., Saitama, Japan). The substrates were treated with ozone (hydrophilic treatment) and HMDS (hydrophobic treatment). Additionally, dextrin-based resist D80-10 and indigestible dextrin-based resist IDex80-10 were spin-coated and baked to form films, and the water contact angles of each sample were measured. Measurements were performed at an ambient temperature of 25 °C, the amount of drop was 1.0 mL, using the 0/2 analysis method. The contact angle was recorded every second for 9 s after film formation. The average value was calculated by excluding the measurements at 0 s and 9 s. Each sample was evaluated thrice.

2.4.2. Exposure Sensitivity Measurement

The solvent was removed by volatilization by spin coating 3 mL of the synthesized positive-type water-developable resist onto a silicon wafer using a spinner (CLEAN TRACK ACT8; Tokyo Electron Limited, Tokyo, Japan) at 3000 rpm for 30 s, followed by baking at 110 °C for 60 s. Subsequently, exposure at 1000 mJ/cm^2 was performed using a mask alignment exposure system (LTCET-500: Lithotech Japan, Saitama, Japan) and a sensitivity verification mask (Taiyo-ink Corporation, Saitama, Japan: 5-inch Multi-Transmission Mask). After immersion in deionized water for 1 min, the water was removed by baking at 80 °C for 60 s. Exposure sensitivity was confirmed by measuring the film thickness before and after development of the film.

2.4.3. Measurement of Film Thickness Variation with Development Time

The synthesized water-developable positive-type resist (D80-10 and IDex80-10) was dispensed onto silicon wafers. Spin coating was performed at 3000 rpm for 30 s using a spinner, followed by baking at 110 °C for 60 s to volatilize and remove the solvent. Subsequently, exposure was performed using a mask-adhering exposure apparatus at 150 mJ/cm^2 for D80-10 and 130 mJ/cm^2 for IDex80-10. The water was removed by immersion in deionized water for 3, 5, 15, or 30 s, followed by baking at 80 °C for 60 s. The development rate was confirmed by measuring the film thickness before and after development.

2.5. Spin-Coating, Water Developable Processes in Eco-Friendly Photolithography and Microfabrication Methods

Figure 1 shows the process of green photolithography using the positive-type water-developable resist adopted in this study. Three milliliters of the water-developable resist was dispensed onto a Si wafer treated with hydrophobic treatment (HDMS treatment), spin-coated at 3000 rpm for 30 s using a spinner (CLEAN TRACK ACT8; Tokyo Electron Limited, Tokyo, Japan), and baked at 110 °C for 60 s to remove the solvent by volatilization. Next, using a mask alignment exposure system (LTCET-500: Lithotech Japan, Saitama, Japan) and a resolution verification mask (TOPPAN PRINTING Co., Ltd., Tokyo, Japan: TOPPAN-TEST-CHART-NO1-PN), exposure was performed at 150 mJ/cm^2 for D80-10 and 130 mJ/cm^2 for IDex80-10. After soaking in deionized water for 1 min, water was removed by baking at 80 °C for 60 s. The method was used to fabricate line-and-space patterns of positive-type water-developable resist on Si wafers, which were then observed using a confocal laser microscope (Lasertec, Kanagawa, Japan, OPTELICS H1200).

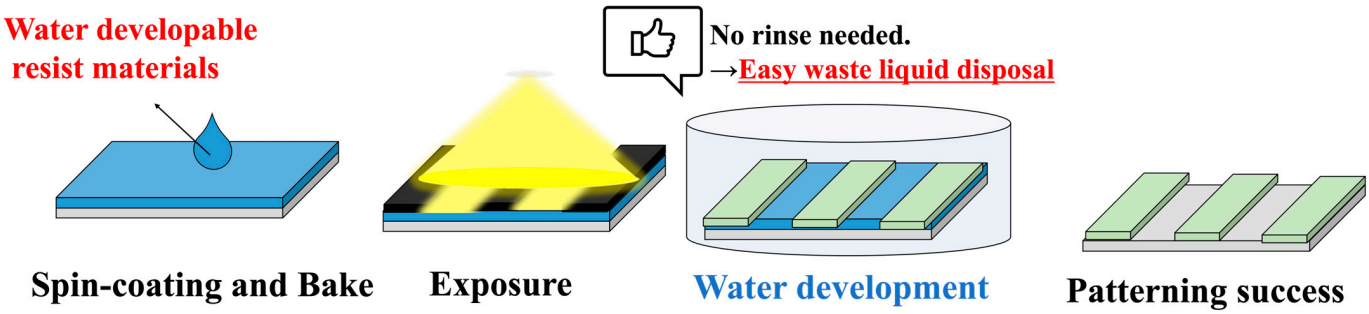


Figure 1. Environmentally friendly photolithography process using positive-type water-developable resist.

3. Results and Discussions

3.1. Chemical Characterization of Materials

In this study, the samples were prepared and analyzed by varying the protection rate and quantities of the PAG and acid quencher. Table 2 summarizes the theoretically planned protection group addition rate, the results obtained via ^{13}C-NMR, the weight-average molecular weight (converted to standard polystyrene) measured without the addition of PAG and acid quencher, and the average film thickness following spin coating and baking.

Table 2. Synthesis results of positive-type water-developable resist.

Samples		Protective Group Addition Amount (%)	Protection Rate (%)	Mw	Average Film Thickness (nm)
D80	D80-5 D80-10	80	72.5	19,700	612 632
D100	D100-5 D100-10	100	93.6	22,500	1052 1071
IDex80	IDex80-5 IDex80-10	80	73.5	2600	598 589
IDex100	IDex100-5 IDex100-10	100	90.8	3600	905 915

Regarding the protection rate of EVE (actual measured value), several factors may account for its reduction compared to the planned protection group addition rate. First, the glycan structure employed as the resist backbone is a water-soluble polymer that

readily retains water within its molecules. This moisture may have deactivated some of the EVE [34]. Additionally, NMP [35] used as a solvent is a polar, non-protonic solvent, which may have influenced the proton transfer rates and reaction equilibrium, potentially diminishing the reaction efficiency [36]. Moreover, the composition of the liquid phase significantly contributes to the selectivity and efficiency of acid-catalyzed reactions [37], and this factor may have also contributed to the decrease in the protection rate.

The weight-average molecular weight was higher for dextrin and lower for indigestible dextrin. Furthermore, when comparing samples with the same protection rate after spin coating and baking, samples with higher molecular weights exhibited greater average film thicknesses and superior film-forming properties.

The FT-IR spectra are shown in Figure 2. The chemical structure changes before and after D80-10 exposure are shown in Figure 2a. A comparison of the spectrum before exposure Figure 2b with the spectrum after exposure (c) revealed a decrease in the C-O bond of the protecting group in Figure 2c after exposure, along with a reduction in the peak of the CH3 group also contained within the protecting group. Furthermore, the peak of the ether group within the cyclic structure [38,39] showed no significant change. This confirmed that the deprotection reaction proceeded upon exposure.

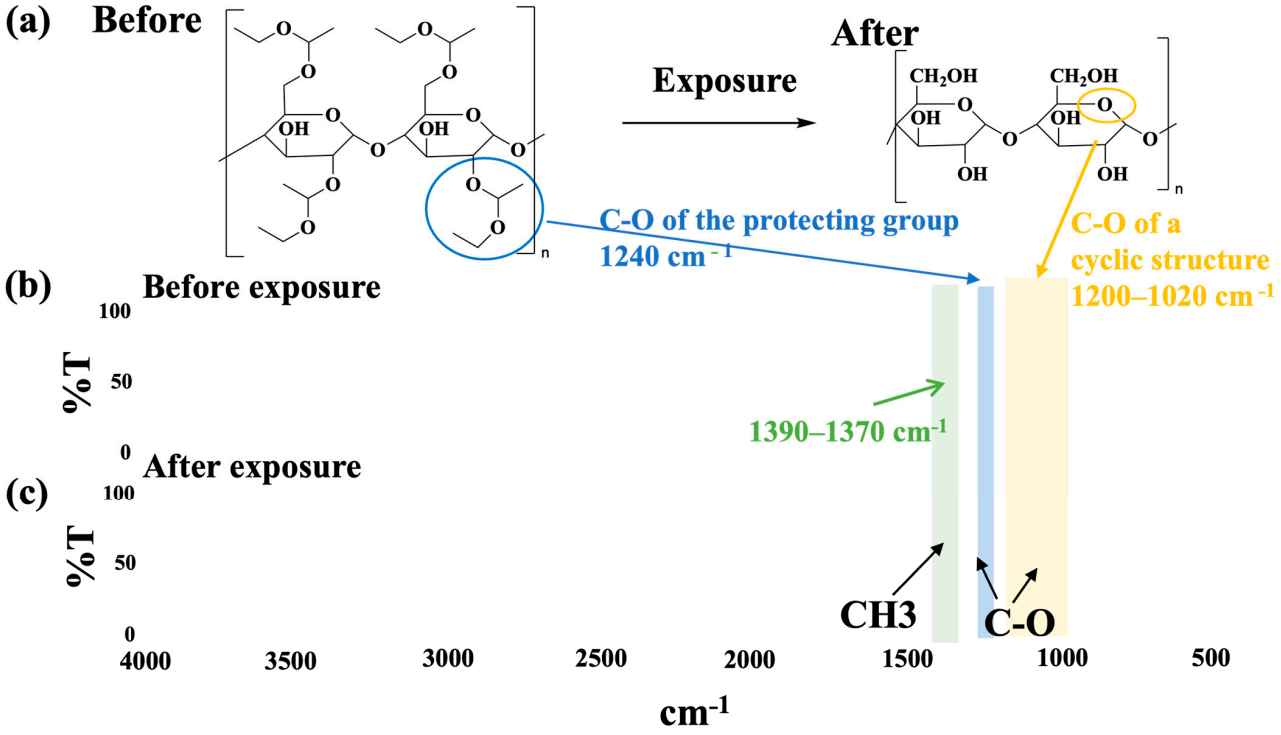


Figure 2. FT-IR measurement results: (**a**) structural changes before and after exposure; (**b**) spectrum before exposure; (**c**) spectrum after exposure.

3.2. Material Property Evaluation

3.2.1. Evaluation of Affinity Between Resist and Substrate

Contact angle measurements were employed to assess the affinity of positive-type water-developable resist towards water and the wettability of the substrate surface, thereby evaluating substrate processing methods. Figure 3 presents the water contact angle measurement results for the positive-type water-developable resists (D80-10 and IDex80-10) examined in this study, alongside the ozone-treated and HMDS-treated substrates. The water contact angles for the positive water-developable resists were 56.3° for D80-10 and 43.9° for IDex80-10. The lower water contact angle of IDex80-10, which has a lower molecular weight, is attributed to its higher solubility in water. Conversely, the water contact angles

of the substrates were 13.9° for the ozone-treated substrate and 75.1° for the HMDS-treated substrate. The HMDS-treated substrate exhibited a contact angle that was more closely aligned with that of the positive-type water-developable resist. Therefore, based on the adhesion between the substrate and the positive water-developable resist, the affinity is deemed higher for the HMDS-treated substrate.

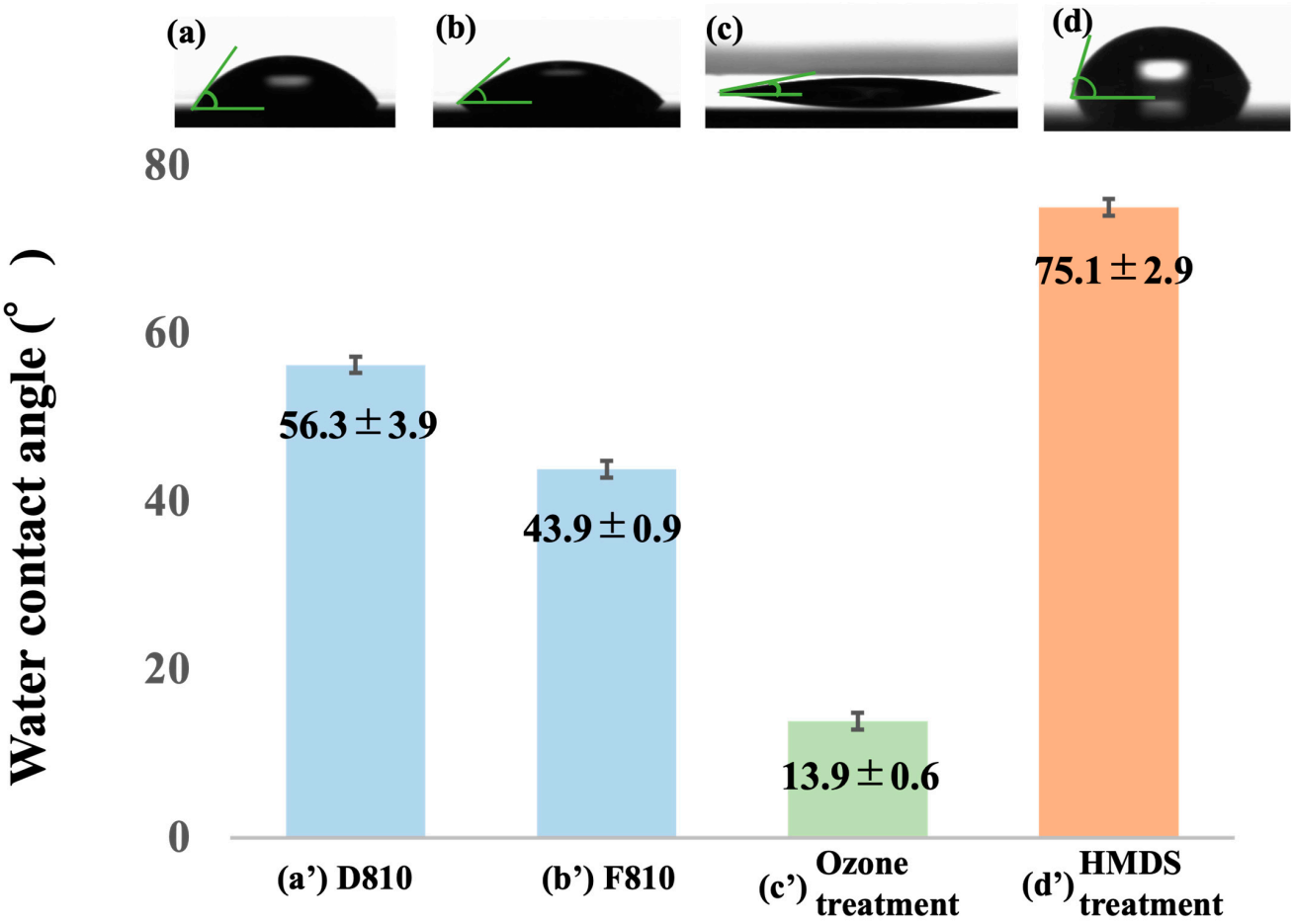


Figure 3. Results of water contact angle measurements. (**a**–**d**) show the water contact angle images, and (**a′**–**d′**) present the corresponding measured values. Data are presented as mean ± SD (n = 3). Each bar represents the mean of three independent experiments, and error bars indicate standard deviation: (**a**,**a′**) dextrin-based resist D80-10; (**b**,**b′**) indigestible dextrin-based resist IDex80-10; (**c**,**c′**) ozone treatment for hydrophilic modification; (**d**,**d′**) HMDS treatment for hydrophobic modification.

In the spin-coating process, an enhanced affinity between the substrate and resist facilitates a more uniform coating. Conversely, during development, if the wettability between the substrate and developer solution surpasses the adhesion between the substrate and resist, insoluble unexposed areas may peel off or collapse. Conversely, if adhesion between the substrate and resist prevails, the pattern remains stable, but residues may persist in exposed areas. Given that the positive-type water-developable resist used in this study exhibited relatively hydrophobic behavior, hydrophilic substrates allowed the developer to penetrate the interface more readily, potentially promoting pattern delamination. Therefore, hydrophobizing the substrate surface via HMDS treatment was determined to enhance the adhesion between the resist and substrate during development, thereby enabling stable pattern formation.

Furthermore, the resist employed in this study utilized PGMEA as its solvent, which is considered to possess higher volatility and improved coating properties compared to conventional water-developable resists [40]. Consequently, in this study, the substrate treat-

ment was determined to be HMDS treatment, prioritizing adhesion during development over wettability during coating.

3.2.2. Exposure Sensitivity Evaluation

Figure 4 presents the exposure sensitivity of positive-type water-developable resists: (a) dextrin-based resist and (b) indigestible dextrin-based resist. Within the dextrin-based series, D80-10 exhibited the highest exposure sensitivity, reaching 140 mJ/cm^2. In the category of indigestible dextrin resists, IDex80-10 exhibited the highest exposure sensitivity at 130 mJ/cm^2. Exposure sensitivity refers to the exposure level at which the residual film thickness reaches 0 ± 10 nm. In both instances, the protection rate was low, indicating that increased amounts of PAG and acid quencher enhanced the sensitivity. These findings suggest a correlation between low protection rates and improved exposure sensitivity. Specifically, for a given amount of PAG, a higher protection rate implies that more time is required for the complete deprotection of all the protecting groups. Furthermore, some reports suggest that lower protection rates are associated with higher resolutions [41]. Therefore, the high sensitivity observed in samples with low protection rates in this study was likely due to the rapid progression of the deprotection reaction. This underscores the necessity of optimizing the protection rate to achieve both exposure sensitivity and high resolution. Additionally, when comparing the dextrin-based resist with the indigestible dextrin-based resist, the latter exhibited a lower minimum exposure amount and higher sensitivity than the former. This difference was attributed to the molecular weight. As indicated in Table 3, indigestible dextrin has a smaller molecular weight than dextrin, suggesting higher solubility in water. Consequently, it is presumed to dissolve more readily in water during development, thereby enhancing the exposure sensitivity.

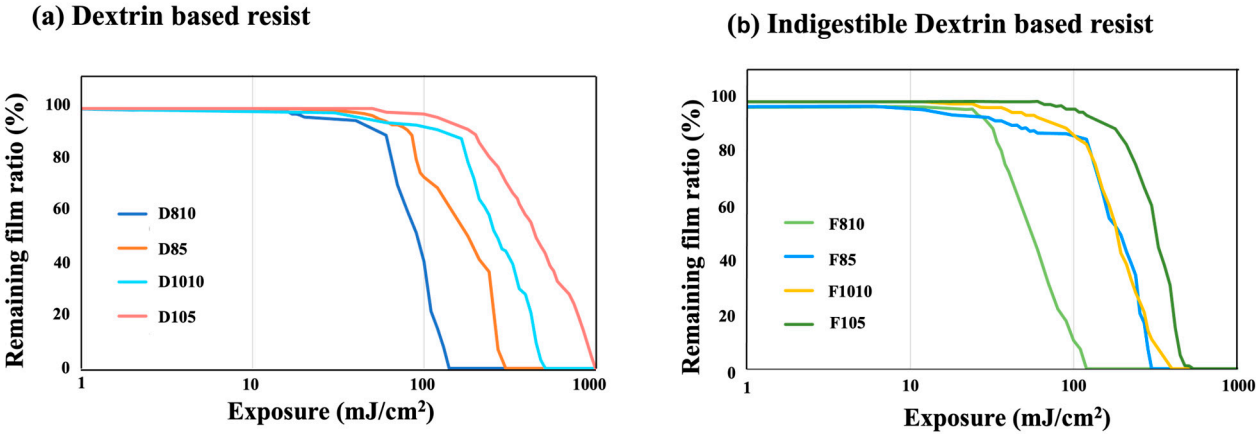


Figure 4. Exposure sensitivity of positive-type water-developable resists: (**a**) 4 samples with different protection rates, PAG, and acid quencher amounts for dextrin-based resist, (**b**) 4 samples with different protection rates, PAG, and acid quencher amounts for indigestible dextrin-based resist.

Table 3. Molecular weight and exposure sensitivity.

Samples	Mw	Exposure Sensitivity (mJ/cm^2)
D80-5	19,700	300
D80-10		140
D100-5	22,500	1000
D100-10		510
IDex80-5	2600	300
IDex80-10		130
IDex100-5	3600	540
IDex100-10		400

3.2.3. Evaluation of Film Thickness Variation with Development Time

The results of the development speed measurements, as presented in Table 4, reveal that the initial film thickness of D80-10 was 632 nm. Through water development, this thickness was reduced to 0 nm within 30 s, and the residual film thickness could be controlled to 10 nm or less within 15 s. Furthermore, for IDex80-10, the initial film thickness was 589 nm, which was reduced to 0 nm within 15 s by aqueous development, and the residual film thickness could be controlled to below 10 nm within 3 s. Therefore, the reduction in film thickness with development time was more rapid for low-molecular-weight, indigestible-dextrin-based resists. While a higher molecular weight enhances the film formation properties, it was also found that the exposure sensitivity and development speed deteriorate owing to the reduced water solubility.

Table 4. Variation in sample film thickness during development.

Samples		D80-10	IDex80-10
initial thickness (nm)		632	589
Film thickness after development (nm)	3 s later	138.7	9.1
	5 s later	27.0	7.1
	15 s later	5.7	0
	30 s later	0	0

3.3. Photolithography and Microfabrication Evaluation

Figure 5 shows the pattern images of (a) D80-10 dextrin-based resist and (b) IDex80-10 indigestible dextrin-based resist, both of which are positive-type water-developable resists. (a1) and (b1) show the horizontal lines for each pattern, while (a2) and (b2) show the vertical lines. The resist pattern formed on the silicon wafer through exposure using a resolution verification mask was examined using a confocal laser microscope. The bright areas in the image represent the silicon substrate (where the resist was developed), and the dark areas indicate the remaining resist film. (c), (d), and (e) show the results of measuring the center, edge, and long side lengths for the horizontal line pattern in (a1) and (b1) and the vertical line pattern in (a2) and (b2), in the lower rows of (a) and (b), respectively. Each average value is displayed, with error bars indicating the standard deviation. For the 3.5 μm mask patterns in (a) D80-10 and (b) IDex80-10, (a) exhibits 3.6 μm and (b) exhibits 3.7 μm, indicating that the pattern has blurred due to development. In the (c) center area, the pattern of IDex80-10 appeared larger and more blurred compared to that of D80-10. In addition, the error bars for IDex80-10 were larger, suggesting lower pattern reproducibility during the development process. In the (d) edge area, the patterns became narrower than those in the center, and the error bars were also larger. This indicates that the edge region exhibited rounding and incomplete development compared to the center. In the (e) long side, no significant difference was observed between D80-10 and IDex80-10.

Table 5 illustrates the relationships between the material, exposure dose, resolution, and molecular weight. The higher resolution observed in the dextrin-based resist in (a) is attributed to its high molecular weight. Lower molecular weights enhance water solubility, thereby improving exposure sensitivity. However, during development, this solubility may have led to the dissolution of unexposed areas in water. This phenomenon is further explained by the fact that the indigestible dextrin-based resist demonstrated a lower water contact angle, as shown in Figure 3 (Section 3.2.1), and a higher affinity for water during contact angle measurements. In essence, while exposure sensitivity can be modulated by the molecular weight, the resolution deteriorates as the molecular weight decreases and the exposure sensitivity increases, indicating a trade-off relationship. Furthermore, it became clear that when the protection rate is high, not only the sensitivity decreases, but the

resolution also deteriorates. With D100-10, the line width was significantly narrower than the target width, resist residue remained on the exposed area, and the pattern was not fully formed even after development. Conversely, with IDex100-10, excessive dissolution during development caused the pattern width to expand, resulting in a line width larger than the target width. These results demonstrate that the protection rate significantly impacts the stability and shape reproducibility of the resist during the development process.

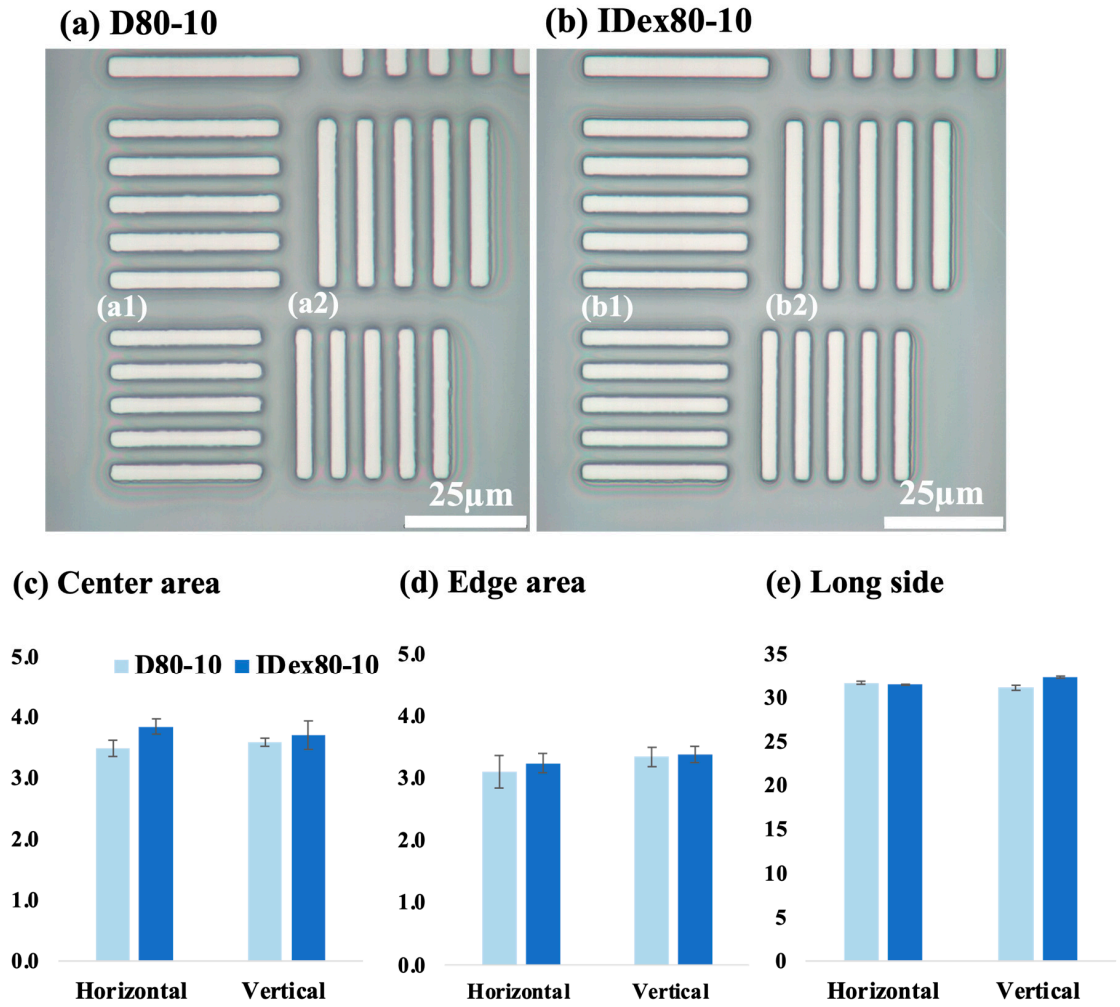


Figure 5. Pattern results: (**a**) D80-10 results, 3.6 µm line pattern, (**a1**) Horizontal line of D80-10, (**b1**) D80-10 vertical line, (**b**) IDex80-10 results, 3.7 µm line pattern, (**a2**) Horizontal line of D80-10, (**b2**) D80-10 vertical line. Resolution comparison. Data are presented as mean ± SD (n = 5). Each bar represents the mean of three independent experiments, and error bars indicate standard deviation: (**c**) center-part, (**d**) edge-part, (**e**) long side.

Table 5. Relationship between materials, exposure dose, resolution, and molecular weight.

Material	Protection Rate (%)	Exposure Dose (mJ/cm^2)	Resolution (µm) (Mask Size: 3.5 µm)	Mw	Remarks
D80-10	72.5	150	3.6	19,700	Good resolution, low sensitivity
IDex80-10	73.5	130	3.7	2600	Low resolution, high sensitivity
D100-10	93.6	510	2.9	22,500	Incomplete pattern formation
IDex100-10	90.8	400	4.4	3600	Pattern broadening

4. Conclusions

In this study, we developed positive-type water-developable resist materials using dextrin and indigestible dextrin as the foundational structure and investigated the effects of coverage rate, photoacid generator (PAG), acid quencher quantity, and molecular weight. The findings indicate that systems incorporating low-molecular-weight indigestible dextrin exhibit faster development and heightened sensitivity, albeit at the expense of reduced resolution, underscoring the necessity of balancing molecular weight, solubility, and resolution. In particular, successful patterning was achieved with D80-10 and IDex80-10 formulations, exhibiting sensitivities of 150 mJ/cm^{-2} and 130 mJ/cm^{-2}, respectively. Furthermore, materials with high sensitivity can be achieved at low protection rates, with additional sensitivity enhancements attainable through the optimization of the PAG and acid quencher quantities. These results suggest that PFAS-free positive-type water-developable resists derived from sugar chains could serve as environmentally friendly photolithography materials, potentially supplanting traditional photoresists that depend on organic solvents by fine-tuning the balance between exposure sensitivity, resolution, and film-forming properties of the resist. This study provides design guidelines for naturally derived positive-type water-developable resists and proposes potential applications not only in electronics but also, owing to their water-developable nature, in life sciences and regenerative medicine.

Author Contributions: Conceptualization, Y.H. and S.T.; data curation, Y.H. and S.T.; formal analysis, T.O., H.H., M.A., M.O. and M.M.; funding acquisition, S.T. and Y.H.; investigation, T.O., M.A., H.H., M.O., M.M., A.M.H., N.H.A. and S.T.; methodology, H.H., M.A., M.O., M.M., T.O., A.M.H., N.H.A. and S.T.; project administration, S.T.; resources, S.T.; supervision, S.T.; validation, H.H., M.A., M.O.,M.M. and S.T.; writing—original draft preparation, Y.H. and S.T.; writing—review and editing, Y.H. and S.T. All authors have read and agreed to the published version of the manuscript.

Funding: The authors wish to acknowledge the funding received from TOBE MAKI Scholarship Foundation 2023–2025, Murata Science and Education Foundation 2025, Japan Society for the Promotion of Science Bilateral Joint Research Projects No. 120259947, Die and Mould Technology Promotion Foundation 2025, Fuji Seal Foundation 2025, Ame Hisaharu Foundation 2025, and Nakato Scholarship Foundation 2024–2025.

Institutional Review Board Statement: Not applicable.

Informed Consent Statement: Not applicable.

Data Availability Statement: The datasets generated and/or analyzed during the current study are not publicly available because they belong to ongoing research but are available from the corresponding author upon reasonable request.

Acknowledgments: This work was supported through the provision of materials and kind guidance from the Technical Development Department of Gunei Chemical Industry, as well as through the valuable practical contributions of the Toyama Industrial Technology Research and Development Center.

Conflicts of Interest: Author Takayuki Ota was employed by the company Gunei Chemical Industry. The remaining authors declare that the research was conducted in the absence of any commercial or financial relationships that could be construed as a potential conflict of interest.

References

1. European Commission. A New Circular Economy Action Plan. EUR-Lex. Available online: https://edz.bib.uni-mannheim.de/edz/doku/wsa/2020/ces-2020-1189-en.pdf (accessed on 24 September 2025).
2. Mubayi, V.; Ahern, C.B.; Calusinska, M.; O'Malley, M.A. Toward a Circular Bioeconomy: Designing Microbes and Polymers for Biodegradation. *ACS Synth. Biol.* **2024**, *13*, 1978–1993. [CrossRef]
3. Langer, R.; Tirrell, D.A. Designing Materials for Biology and Medicine. *Nature* **2004**, *428*, 487–492. [CrossRef]
4. Semenok, D.V.; Kruglov, I.A.; Savkin, I.A.; Kvashnin, A.G.; Oganov, A.R. On Distribution of Superconductivity in Metal Hydrides. *Curr. Opin. Solid State Mater. Sci.* **2020**, *24*, 100808. [CrossRef]

5. Castro-Dominguez, B.; Gröls, J.R.; Alkandari, S.; Perge, L.; Sierra-Avila, C.; Ramirez, H.Z.; de Lima Fontes, M.; Yamada, C.; Lazarini, S.C.; Silva, J.M.; et al. Biopolymers and biocomposites: A comprehensive review of feedstocks, functionalities, and advanced manufacturing techniques for sustainable applications. *Biotechnol. Sustain. Mater.* **2025**, *2*, 8. [CrossRef]
6. Rinaudo, M. Chitin and chitosan: Properties and applications. *Prog. Polym. Sci.* **2006**, *31*, 603–632. [CrossRef]
7. Mathers, R.T. How well can renewable resources mimic commodity monomers and polymers? *J. Polym. Sci. Part A Polym. Chem.* **2012**, *50*, 1–15. [CrossRef]
8. Wang, X.L.; Yang, K.K.; Wang, Y.Z. Properties of starch blends with biodegradable polymers. *J. Macromol. Sci. C Polym. Rev.* **2003**, *43*, 385–409. [CrossRef]
9. Klemm, D.; Kramer, F.; Moritz, S.; Lindström, T.; Ankerfors, M.; Gray, D.; Dorris, A. Nanocelluloses: A new family of nature-based materials. *Angew. Chem. Int. Ed.* **2011**, *50*, 5438–5466. [CrossRef] [PubMed]
10. Parthasarathy, V.; Kumar, P.S.; Albert, A.A.; Krishnasamy, S.; Chandrasekar, M. Recent progress in nanocellulose-based biocomposites for bone tissue engineering and wound healing applications. *Carbohydr. Polym.* **2025**, *357*, 123455. [CrossRef] [PubMed]
11. Altyar, A.E.; El-Sayed, A.; Abdeen, A.; Piscopo, M.; Mousa, S.A.; Najda, A.; Abdel-Daim, M.M. Abdel-Daim, Future regenerative medicine developments and their therapeutic applications. *Biomed. Pharmacother.* **2023**, *158*, 114131. [CrossRef] [PubMed]
12. Bettinger, C.J.; Langer, R.; Borenstein, J.T. Engineering substrate topography at the micro- and nanoscale to control cell function. *Angew. Chem. Int. Ed.* **2009**, *48*, 5406–5415. [CrossRef]
13. Discher, D.E.; Janmey, P.; Wang, Y.L. Tissue cells feel and respond to the stiffness of their substrate. *Science* **2005**, *310*, 1139–1143. [CrossRef] [PubMed]
14. Whitesides, G.M. The origins and the future of microfluidics. *Nature* **2006**, *442*, 368–373. [CrossRef] [PubMed]
15. Fruncillo, S.; Su, X.; Liu, H.; Wong, L.S. Lithographic processes for the scalable fabrication of micro- and nanostructures for biochips and biosensors. *ACS Sens.* **2021**, *6*, 2002–2024. [CrossRef] [PubMed]
16. Park, H.S.; Lee, S.Y.; Yoon, H.; Noh, I. Biological evaluation of micro-patterned hyaluronic acid hydrogel for bone tissue engineering. *Pure Appl. Chem.* **2014**, *86*, 1911–1922. [CrossRef]
17. Zhu, S.; Zeng, W.; Meng, Z.; Luo, W.; Ma, L.; Li, Y.; Lin, C.; Huang, Q.; Lin, Y.; Liu, X.Y. Using wool keratin as a basic resist material to fabricate precise protein patterns. *Adv. Mater.* **2019**, *31*, 1900870. [CrossRef]
18. Bhatia, S.N.; Chen, C.S. Tissue engineering at the micro-scale. *Biomed. Microdevices* **1999**, *2*, 131–144. [CrossRef]
19. Edmondson, R.; Broglie, J.J.; Adcock, A.F.; Yang, L. Three-dimensional cell culture systems and their applications in drug discovery and cell-based biosensors. *ASSAY Drug Dev. Technol.* **2014**, *12*, 207–218. [CrossRef]
20. Engler, A.J.; Sen, S.; Sweeney, H.L.; Discher, D.E. Matrix elasticity directs stem cell lineage specification. *Cell* **2006**, *126*, 677–689. [CrossRef]
21. Xia, Y.; Whitesides, G.M. Soft lithography. *Angew. Chem. Int. Ed.* **1998**, *37*, 550–575. [CrossRef]
22. Qin, D.; Xia, Y.; Whitesides, G.M. Soft lithography for micro- and nanoscale patterning. *Nat. Protoc.* **2010**, *5*, 491–502. [CrossRef]
23. Lee, C.H.; Wang, C.L.; Lin, H.F.; Chai, C.Y.; Hong, M.Y.; Ho, C.K. Toxicity of tetramethylammonium hydroxide: Review of two fatal cases of dermal exposure and development of an animal model. *Toxicol. Ind. Health* **2011**, *27*, 497–503. [CrossRef]
24. Morikawa, J.; Ryu, M.; Maximova, K.; Balčytis, A.; Seniutinas, G.; Fan, L.; Mizeikis, V.; Li, J.; Wang, X.; Zamengo, M.; et al. Silk fibroin as a water-soluble bio-resist and its thermal properties. *RSC Adv.* **2016**, *6*, 11863–11869. [CrossRef]
25. Park, J.; Lee, S.G.; Marelli, B.; Lee, M.; Kim, T.; Oh, H.K.; Jeon, H.; Omenetto, F.G.; Kim, S. Eco-friendly photolithography using water-developable pure silk fibroin. *RSC Adv.* **2016**, *6*, 39330–39334. [CrossRef]
26. Servin, I.; Teolis, A.; Bazin, A.; Durin, P.; Sysova, O.; Gablin, C.; Saudet, B.; Leonard, D.; Soppera, O.; Leclercq, J.-L.; et al. Water-soluble bio-sourced resists for DUV lithography in a 200/300 mm pilot line environment. *Micro Nano Eng.* **2023**, *19*, 100202. [CrossRef]
27. Kotthoff, M.; Müller, J.; Jürling, H.; Schlummer, M.; Fiedler, D. Perfluoroalkyl and polyfluoroalkyl substances in consumer products. *Environ. Sci. Pollut. Res.* **2015**, *22*, 14546–14559. [CrossRef]
28. Cousins, I.T.; DeWitt, J.C.; Glüge, J.; Goldenman, G.; Herzke, D.; Lohmann, R.; Ng, C.A.; Scheringer, M.; Wang, Z. The high persistence of PFAS is sufficient for their management as a chemical class. *Environ. Sci. Process. Impacts* **2020**, *22*, 2307–2312. [CrossRef] [PubMed]
29. Henry, B.J.; Carlin, J.P.; Hammerschmidt, J.A.; Buck, R.C.; Buxton, L.W.; Fiedler, H.; Seed, J.; Hernandez, O. A critical review of the application of polymer of low concern and regulatory criteria to fluoropolymers. *Integr. Environ. Assess. Manag.* **2018**, *14*, 316–334. [CrossRef]
30. Zhu, S.; Tang, Y.; Lin, C.; Liu, X.Y.; Lin, Y. Recent advances in patterning natural polymers: From nanofabrication techniques to applications. *Small Methods* **2021**, *5*, 2001060. [CrossRef]
31. Chung, S.C.; Park, J.S.; Jha, R.K.; Kim, J.; Kim, J.; Kim, M.; Choi, J.; Kim, H.; Park, D.-H.; Gogurla, N.; et al. Engineering silk protein to modulate polymorphic transitions for green lithography resists. *ACS Appl. Mater. Interfaces* **2022**, *14*, 56623–56634. [CrossRef] [PubMed]

32. Amano, T.; Kobayasi, M.; Takei, S. Micropatterning performance and physical characteristics of water-soluble high molecular weight polysaccharide photoresist materials. *J. Photopolym. Sci. Technol.* **2021**, *34*, 181–186. [CrossRef]
33. Hachikubo, Y.; Miura, S.; Yamagishi, R.; Ando, M.; Kobayashi, M.; Ota, T.; Amano, T.; Takei, S. Amylopectin-based eco-friendly photoresist material in water-developable lithography processes for surface micropatterns on polymer substrates. *J. Photopolym. Sci. Technol.* **2023**, *36*, 197–204.
34. von Schreeb, A.; Sjöstrand, B.; Ek, M.; Henriksson, G. Drying and hornification of swollen cellulose. *Cellulose* **2025**, *32*, 5179–5189. [CrossRef]
35. Basma, N.S.; Headen, T.F.; Shaffer, M.S.; Skipper, N.T.; Howard, C.A. Local structure and polar order in liquid N-methyl-2-pyrrolidone (NMP). *J. Phys. Chem. B* **2018**, *122*, 8963–8971. [CrossRef]
36. Sen Gupta, S.K. Proton transfer reactions in apolar aprotic solvents. *J. Phys. Org. Chem.* **2016**, *29*, 251–264.
37. Chew, A.K.; Walker, T.W.; Shen, Z.; Demir, B.; Witteman, L.; Euclide, J.; Van Lehn, R.C. Effect of mixed-solvent environments on the selectivity of acid-catalyzed dehydration reactions. *ACS Catal.* **2019**, *10*, 1679–1691.
38. Smith, B.C. An IR spectral interpretation potpourri: Carbohydrates and alkynes. *Spectrscopy* **2017**, *32*, 18–24.
39. Gafour, H.M.; Bouterfas, M.; Bekhti, N.; Derrar, S.N.; Rahal, M.S. Harmonic Dynamics of αD-Lactose in the Crystalline State. *J. Mol. Imaging Dyn.* **2011**, *1*, 1000102.
40. Amano, T.; Hirata, D.; Hasegawa, Y.; Takei, S. Evaluation of Nano-Patterning Performance of Water-Soluble Material for Photoresist Using Sugar Chain. *J. Photopolym. Sci. Technol.* **2020**, *33*, 445–450. [CrossRef]
41. Liu, J.; Kang, W. New Chemically Amplified Positive Photoresist with Phenolic Resin Modified by GMA and BOC Protection. *Polymers* **2023**, *15*, 1598. [CrossRef] [PubMed]

Disclaimer/Publisher's Note: The statements, opinions and data contained in all publications are solely those of the individual author(s) and contributor(s) and not of MDPI and/or the editor(s). MDPI and/or the editor(s) disclaim responsibility for any injury to people or property resulting from any ideas, methods, instructions or products referred to in the content.